

Impact of Magnetic Field on the Onset of Double Diffusive Rayleigh-Benard Convection Governed by Local Thermal Non-Equilibrium in a Double Layered System

R. Sumithra¹, Shyamala Venkatraman^{2*} and R.K. Vanishree³

¹Associate Professor and ²Research Scholar, Department of UG, PG Studies & Research in Mathematics, Government Science College Autonomous, Nrupathunga University, Bengaluru, Karnataka, India. sumitra_diya@yahoo.com and svr02009@gmail.com

³Department of Mathematics, Maharani Science College for Women, Maharani Cluster University, Bengaluru, Karnataka, India.

Abstract

Onset of Double Diffusive Rayleigh-Benard-Magneto (DDRBM) convection is studied for a double layered system composed of incompressible fluid confined by adiabatic rigid peripheries under the governance of Local Thermal Non-Equilibrium (LTNE). Result of the acquired problem is obtained analytically through the mode of Regular Perturbation. Consequence of physical factors such as solid phase thermal expansion ratio, solid phase thermal diffusivity ratio and inter-phase thermal diffusivity ratio that favours LTNE are being analysed. The outcome of altering the constraints namely fluid phase thermal expansion ratio, solute Rayleigh number, Chandrasekhar number, thermal ratio, concentration ratio, fluid phase solute diffusivity ratio, solute diffusivity ratio in fluid layer and porous layer subject to LTNE set-up are paralleled with that of LTE set-up with diagrammatic representation.

Keywords: Local Thermal Non-Equilibrium (LTNE), Magnetic Field, Double Layered System, Mode of Regular Perturbation.

Nomenclature:

English letters			
$\vec{q}_{fl} = (u_F, v_F, w_F)$: velocity vector	C_p	: specific heat capacity
t	: time	C_F, C_P	: concentrations
P_F & P_P	: pressure	\hat{S}	: salinity ratio
g	: acceleration due to gravity	C_0	: Interface species concentration
T_F, T_{fp} & T_{sp}	: temperatures	h	: inter-phase heat transfer coefficient
T_0	: interface temperature	a_F & a_P	: non dimensional horizontal wave numbers
K	: permeability		

English letters			
n_F & n_P	: frequencies	H	: scaled inter-phase heat transfer coefficient
W_F & W_P	: dimensionless vertical velocities	\hat{T}	: thermal ratio
$R_{F'}$, $R_{T_{f'}}$, $R_{T_{sP'}}$, R_{SF} & R_{SP}	: Rayleigh numbers, defined below	\hat{d}	: depth ratio
Greek Symbols			
ρ_0	: reference density	$\hat{\kappa}_{fp}$ & $\hat{\kappa}_{sP}$: thermal diffusivity ratio
μ	: fluid viscosity	β	: porous parameter
ρ_F & ρ_P	: fluid density	β^2	: Darcy number
$\kappa_{F'}$, κ_{fp} & κ_{sP}	: thermal diffusivities	τ	: inter-phase thermal diffusivity ratio
κ_{cF} & κ_{cP}	: solute diffusivities	τ_{cF} & τ_{cP}	: solute diffusivity ratios
$\alpha_{TF'}$, $\alpha_{T_{fp}}$ & $\alpha_{T_{sP}}$: thermal expansion coefficients	$\hat{\mu}$: viscosity ratio
ϕ	: porosity		
ζ_f & ζ_s	: thermal expansion ratio		
Subscripts			
P	: porous medium	S	: solid phase
f	: fluid phase	b	: basic state
F	: Fluid layer		

1. Introduction

The role of double diffusive convection in mineral upsurge is significant. It occupies a major part in salt fingering which in turn is substantial in the climatic regulation. The importance of double diffusive convection spreads into various natural and applied processes namely astrophysics, geology, oceanography, metallurgy, crystal production, solar pond, drying processes, engineering etc. Also, Double diffusive convection finds a prominent place in identifying magmas.

Involvement of LTNE is noteworthy in swift flow and existence of grander thermal inclination among fluid and solid phases. Journal bearings, food storage, geothermal energy, pollutant transport underground, crystal growth are some of the systems where composite layer set up conquers a protuberant position. Numerous literatures are available on double diffusive convection on single layer influenced by magnetic field. Sumithra & Manjunatha have investigated the single component convection in a composite layer under the impact of magnetic field in

[2012] and double diffusive magneto convection in a double layer in [2018]. A very scrimpy attention was given to research over double diffusive convection in a composite layer under Local Thermal Non-Equilibrium conditions in the presence of magnetic field.

Herbert & Stewart [1981] provided a review on essential advances in double diffusive convection. Ehrenstein & Peyret [1989] studied a Chebyshev collocation method aimed at Navier-Stokes equations considering application to double-diffusive convection. Hughes & Weiss [1995] examined double diffusive convection taking two stabilizing gradients into account and analysed the weird results of magnetic buoyancy. Galenko & Danilov [1997] investigated local non equilibrium on rapid dendritic growth in a binary alloy melt. Srinivasacharya & Swami [2012] investigated Double Diffusive Natural Convection with respect to Power-Law Fluid Saturated Porous Medium under Soret and Dufour Effects.

Pascale [2017] reviewed double diffusive convection at low Prandtl numbers. Asha & Sunitha [2020] examined double diffusion on peristaltic flow of nanofluid under the influences of magnetic field,

porous medium, and thermal radiation. Shashi Prabha et al [2020] analysed the heat transfer through mixed convection boundary layer in a porous medium under LTNE conditions. Abdalraheem et al [2021] studied double diffusion in a nanofluid cavity with a wavy hot source subjected to a magnetic field using ISPH method. Muhammad et al [2022] investigated double diffusive magneto-free-convection flow of Oldroyd-B fluid over a vertical plate under the influence of heat and mass flux.

Enthused by the above survey of literatures, the present paper analyses the onset of Magnetic Field dominated Double Diffusive Rayleigh-Benard (DDRBM) convection for a double layered system under the governance of Local Thermal Non-Equilibrium (LTNE). Consequence of physical factors such as solid phase thermal expansion ratio, solid phase thermal diffusivity ratio and inter-phase thermal diffusivity ratio that favours LTNE are being analysed. The outcome of altering the constraints namely fluid phase thermal expansion ratio, solute Rayleigh number, Chandrasekhar number, thermal ratio, concentration ratio, fluid phase solute diffusivity ratio, solute diffusivity ratio in fluid layer and porous layer subject to LTNE set-up are paralleled with that of LTE set-up with diagrammatic representation.

2. Mathematical formulation

An infinite horizontal layer involving incompressible, Boussinesq fluid holding thickness d_F is considered. Densely packed porous layer saturated with same fluid with thickness d_p lies beneath the fluid layer levied with magnetic field of intensity H_0 in the perpendicular z-direction. The precinct below the porous layer is presumed to be rigid and that above the fluid layer is

presumed to be free from surface tension effects based on temperature. A Cartesian coordinate system as in the case of Sumithra [2014], Sumithra and Shyamala [2020] in which the origin is placed at the interface between fluid and porous layers and the z-axis pointing upright is considered. For the porous layer, solid phase as well as the fluid phase are purported to be in LTNE and a solid-fluid field model is considered to express distinctly the temperatures with regard to the solid and fluid phases. The equations acquired pertaining to the present research problem are

In $0 \leq z_F \leq 1$

$$(D^2 - a_F^2)^2 W_F = R_F a_F^2 \theta_F - R_{SF} a_F^2 S_F + Q_F D^2 W_F \dots (1)$$

$$(D^2 - a_F^2) \theta_F + W_F = 0 \dots (2)$$

$$\tau_{cF} (D^2 - a_F^2) S_F + W_F = 0 \dots (3)$$

In $0 \leq z_P \leq 1$

$$(D_p^2 - a_p^2)^2 W_P = -\beta^2 R_{TF} a_p^2 \theta_{JP} - \beta^2 R_{SP} a_p^2 \theta_P \tau + \beta^2 R_{SP} a_p^2 S_P \tau_{cP} - Q_P \beta^2 D_p^2 W_P \dots (4)$$

$$\phi (D_p^2 - a_p^2) \theta_{JP} + W_P = -H (\theta_{SP} - \theta_{JP}) \dots (5)$$

$$(1 - \phi) (D_p^2 - a_p^2) \theta_{SP} = H (\theta_{SP} - \theta_{JP}) \dots (6)$$

$$\tau_{cP} (D_p^2 - a_p^2) S_P + W_P = 0 \dots (7)$$

For the fluid layer, $R_F = \frac{g \alpha_{TF} (T_0 - T_U) d_F^3}{\nu_1 \kappa_F}$

is the thermal Rayleigh number and

$R_{SF} = \frac{g \alpha_{SF} (C_0 - C_U) d_F^3}{\nu_1 \kappa_F}$ is the solute Rayleigh number. For the porous layer,

$R_{TF} = \frac{g \alpha_{TF} (T_L - T_0) d_P^3}{\nu_1 \kappa_{JP}}$ is the fluid phase Rayleigh

2. MATHEMATICAL FORMULATION

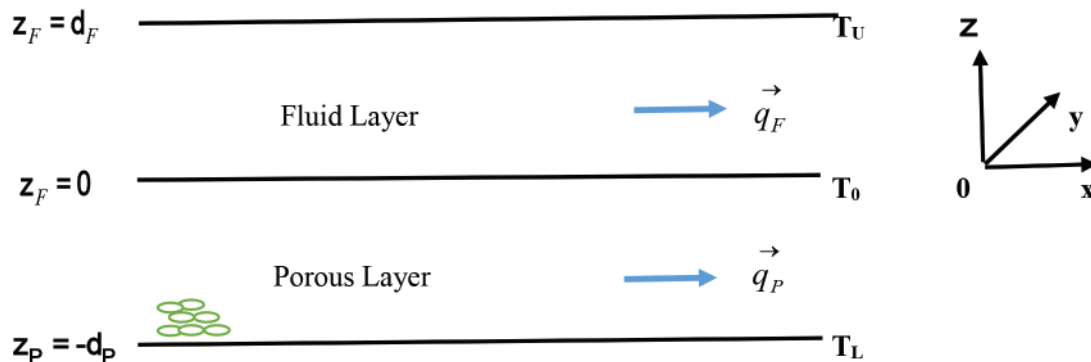


Figure 1: Outline of the Problem

number, $R_{T_{SP}} = \frac{g\alpha_{T_{SP}}(T_L - T_0)d_P^3}{\nu\kappa_{SP}}$ is the solid phase Rayleigh number, $R_{SP} = \frac{g\alpha_{SF}(T_L - T_0)d_P^3}{\nu\kappa_{SP}}$ is the solute Rayleigh number, $\beta^2 = \frac{K}{d_P^2} = Da$ represents Darcy number, $\tau = \frac{\kappa_{SP}}{\kappa_{FP}}$ represents ratio of thermal diffusivity of the solid phase to fluid phase, $\tau_{cF} = \frac{\kappa_{cF}}{\kappa_F}$ is the ratio of solute diffusivity to the thermal diffusivity in fluid layer, $\tau_{cP} = \frac{\kappa_{cP}}{\kappa_{FP}}$ is the ratio of solute diffusivity to the thermal diffusivity with respect to fluid in the porous layer, $H = \frac{hd_P^2}{\kappa_{FP}}$ is the scaled inter-phase heat transfer coefficient.

Equations (1) to (7) are ordinary differential equations of eighteenth order and required to be solved using the following boundary conditions as performed in Sumithra et. al [2021].

3. Boundary conditions

Normal mode expansion performed on the appropriate boundary conditions after non dimensionalization. They are

$$\begin{aligned} W_F(1) &= 0, \quad DW_F(1) = 0, \quad D\theta_F(1) = 0, \quad DS_F(1) = 0, \\ \hat{T}W_F(0) &= W_P(1), \quad \hat{T}\hat{d}DW_F(0) = \hat{\mu}DW_P(1) \\ \theta_F(0) &= \hat{T}\theta_{FP}(1), \quad \theta_F(0) = \hat{T}\theta_{SP}(1), \quad D\theta_F(0) = D\theta_{FP}(1), \quad D\theta_F(0) = D\theta_{SP}(1) \\ S_F(0) &= \hat{S}S_P(1), \quad DS_F(0) = DS_P(1) \\ \hat{T}\hat{d}^3\beta^2[D^3W_F(0) - 3a_F^2DW_F(0)] &= -DW_P(1) + \hat{\mu}\beta^2[D^3W_P(1) - 3a_P^2DW_P(1)] \\ \hat{T}\hat{d}^2(D^2 + a_F^2)W_F(0) &= \hat{\mu}(D^2 + a_P^2)W_P(1) \\ W_P(0) &= 0, \quad DW_P(0) = 0, \quad D\theta_{FP}(0) = 0, \quad D\theta_{SP}(0) = 0, \quad DS_P(0) = 0 \end{aligned}$$

Where $\hat{T} = \frac{T_L - T_0}{T_0 - T_U}$ is the thermal ratio, $\hat{S} = \frac{C_L - C_0}{C_0 - C_U}$ is the solute ratio, $\beta = \sqrt{\frac{K}{d_P^2}}$, $\hat{d} = \frac{d_P}{d_F}$ is the depth ratio and $\hat{\mu} = \frac{\mu_P}{\mu_F}$ is the viscosity ratio.

4. Solving using regular perturbation method

At boundaries with constant heat dissipation, convection occurs at smaller horizontal wave number ' a_F '. Hence we expand

$$\begin{bmatrix} W_F \\ \theta_F \\ S_F \end{bmatrix} = \sum_{j=0}^{\infty} a_F^{2j} \begin{bmatrix} W_{Fj} \\ \theta_{Fj} \\ S_{Fj} \end{bmatrix} \quad \text{and} \quad \begin{bmatrix} W_P \\ \theta_{FP} \\ \theta_{SP} \\ S_P \end{bmatrix} = \sum_{j=0}^{\infty} a_P^{2j} \begin{bmatrix} W_{Pj} \\ \theta_{FPj} \\ \theta_{SPj} \\ S_{Pj} \end{bmatrix}$$

The solutions of zero order equations are obtained using an arbitrary factor and are

$$W_{F0}(z_F) = 0, \quad \theta_{F0}(z_F) = \hat{T}, \quad W_{P0}(z_P) = 0, \quad \theta_{FP0}(z_P) = 1, \quad \theta_{SP0}(z_P) = 1, \quad S_{F0}(z_F) = \hat{S}, \quad S_{P0}(z_P) = 1$$

The first order equations in a_F^2 are:

For fluid layer,

$$D^4W_{F1} - Q_F D^2W_{F1} - R_F \hat{T} + R_{SF} \hat{S} = 0 \quad \dots (8)$$

$$D^2\theta_{F1} - \hat{T} + W_{F1} = 0 \quad \dots (9)$$

$$\tau_{cF} D^2 S_{F1} - \tau_{cF} \hat{S} + W_{F1} = 0 \quad \dots (10)$$

For porous layer,

$$D^2 W_{P1} + Q_P \beta^2 D^2 W_{P1} + \beta^2 R_{T_{FP}} + \beta^2 R_{T_{SP}} \tau - \beta^2 R_{SP} \tau_{cP} = 0 \quad \dots (11)$$

$$(\phi D^2 - H)\theta_{fP1} + H\theta_{sP1} + W_{P1} - \phi = 0 \quad \dots (12)$$

$$[(1 - \phi)D^2 - H]\theta_{sP1} + H\theta_{fP1} - (1 - \phi) = 0 \quad \dots (13)$$

$$\tau_{cP} D^2 S_{P1} - \tau_{cP} + W_{P1} = 0 \quad \dots (14)$$

The corresponding boundary conditions are

$$W_{F1}(1) = 0, \quad DW_{F1}(1) = 0, \quad D\theta_{F1}(1) = 0, \quad DS_{F1}(1) = 0$$

$$\hat{T}W_{F1}(0) = \hat{d}^2 W_{P1}(1), \quad \hat{T}DW_{F1}(0) = \hat{\mu} \hat{d} DW_{P1}(1)$$

$$\theta_{F1}(0) = \hat{T} \hat{d}^2 \theta_{fP1}(1), \quad \theta_{F1}(0) = \hat{T} \hat{d}^2 \theta_{sP1}(1)$$

$$D\theta_{F1}(0) = \hat{d}^2 D\theta_{fP1}(1), \quad D\theta_{F1}(0) = \hat{d}^2 D\theta_{sP1}(1)$$

$$S_{F1}(0) = \hat{S} \hat{d}^2 S_{P1}(1), \quad DS_{F1}(0) = \hat{d}^2 DS_{P1}(1)$$

$$\hat{T} \hat{d} \beta^2 D^3 W_{F1}(0) = -DW_{P1}(1) + \hat{\mu} \beta^2 D^3 W_{P1}(1), \quad \hat{T} D^2 W_{F1}(0) = \hat{\mu} D^2 W_{P1}(1)$$

$$W_{P1}(0) = 0, \quad DW_{P1}(0) = 0, \quad D\theta_{fP1}(0) = 0, \quad D\theta_{sP1}(0) = 0, \quad DS_{P1}(0) = 0$$

W_{F1} and W_{P1} are obtained by solving equations (8) & (11) and are

$$W_{F1}(z_F) = B_1 + B_2 z_F + B_3 \text{Cosh}[\sqrt{Q_F} z_F] + B_4 \text{Sinh}[\sqrt{Q_F} z_F] - (R_F \hat{T} - R_{SF} \hat{S}) \frac{z_F^2}{2Q_F} \quad \dots (15)$$

$$W_{P1}(z_P) = B_5 + B_6 z_P - \frac{\beta^2 R_{T_{FP}} + \beta^2 R_{T_{SP}} \tau - \beta^2 R_{SP} \tau_{cP}}{2(1 + Q_P \beta^2)} z_P^2 \quad \dots (16)$$

Where the constants B_1, B_2, B_3, B_4, B_5 & B_6 evaluated using velocity boundary conditions are

$$B_1 = A_1 \left[A_2 + \frac{\text{Coth}[\sqrt{Q_F}]}{Q_F \sqrt{Q_F}} \left(\frac{1}{\hat{d} Q_F \sqrt{Q_F}} - A_2 \right) - \frac{\text{Sinh}[\sqrt{Q_F}]}{\hat{d} Q_F \sqrt{Q_F}} \right] + \frac{R_F \hat{T} - R_{SF} \hat{S}}{2Q_F} \left[1 - \frac{2}{\sqrt{Q_F} \text{Sinh}[\sqrt{Q_F}]} \right],$$

$$B_2 = A_1 \times A_2, \quad B_3 = \frac{R_F \hat{T} - R_{SF} \hat{S}}{Q_F \sqrt{Q_F} \text{Sinh} \sqrt{Q_F}} - \frac{A_1}{Q_F \sqrt{Q_F} \text{Sinh} \sqrt{Q_F}} \left(\frac{1}{\hat{d} Q_F \sqrt{Q_F}} - A_2 \right), \quad B_4 = \frac{A_1}{\hat{d} Q_F \sqrt{Q_F}},$$

$$A_1 = \frac{R_{SP} \tau_{cP} - R_{T_{FP}} - R_{T_{SP}} \tau}{\hat{T}(1 + Q_P \beta^2)}, \quad A_2 = \frac{1}{\hat{d} Q_F} + \hat{\mu} \hat{d} \beta^2, \quad B_5 = B_6 = 0$$

4.1. Solvability Condition:

The compatibility condition, derived by applying the corresponding boundary conditions to the differential equations with respect to heat and species concentration is

$$(1 + \tau_{cP}) \int_0^1 W_{F1}(z_F) dz_F + \hat{d}^2 (1 + \tau_{cF}) \int_0^1 W_{P1}(z_P) dz_P = (\hat{d}^2 + \hat{T}) + (\hat{d}^2 + \hat{S}) \tau_{cF} \tau_{cP} \quad \dots (17)$$

4.2. Solution:

$W_{F1}(z_{F1})$ & $W_{P1}(z_{P1})$ are substituted in equation (17) and an expression for Critical Rayleigh Number is obtained and is found to be

$$R_{FC} = \frac{(\hat{d}^2 + \hat{T}) + (\hat{d}^2 + \hat{S})\tau_{cF}\tau_{cP} + R_{SF} \left\{ (1 + \tau_{cP})[\delta_{14} - \delta_{15} + \delta_{16}] - \hat{d}^4 \hat{\kappa}_{cP}^2 \tau_{cP} \times \right.}{(1 + \tau_{cP})[\delta_{14} - \delta_{15} + \delta_{16}] - [\zeta_f \hat{\kappa}_{fP}^2 + \zeta_s \hat{\kappa}_{sP}^2 \tau] \hat{d}^4 \times \left. \delta_1 [\delta_2 + \delta_3 + \delta_4 \times \delta_5 - \delta_6 - \delta_7 - \delta_8 \times \delta_5 + \delta_9 - \delta_{10}] \right\}}$$

Where $\delta_1 = \frac{1 + \tau_{cP}}{1 + Q_P \beta^2}$, $\delta_2 = \frac{1}{\hat{d} Q_F \hat{T}}$, $\delta_3 = \frac{\hat{d} \hat{\mu} \beta^2}{\hat{T}}$, $\delta_4 = \frac{\text{Cosh} \sqrt{Q_F}}{\hat{T} Q_F \sqrt{Q_F}}$,

$$\delta_5 = \frac{1}{\hat{d} Q_F \sqrt{Q_F}} - \frac{1}{\hat{d} Q_F} - \hat{d} \hat{\mu} \beta^2$$

$$\delta_6 = \frac{\text{Sinh} \sqrt{Q_F}}{\hat{d} \hat{T} Q_F \sqrt{Q_F}}, \delta_7 = \frac{1}{2 \hat{T}} \left[\frac{1}{\hat{d} Q_F} - \hat{d} \hat{\mu} \beta^2 \right], \delta_8 = \frac{1}{\hat{T} \sqrt{Q_F}}, \delta_9 = \frac{\text{Cosh} \sqrt{Q_F}}{\hat{d} Q_F^2 \hat{T}} - \frac{1}{\hat{d} Q_F^2 \hat{T}},$$

$$\delta_{10} = \frac{\hat{d} (1 + \tau_{cF}) \beta^2}{6 (1 + \tau_{cP})}, \delta_{11} = \frac{\hat{T}}{2 Q_F} \left(1 - \frac{2}{\sqrt{Q_F} \text{Sinh} \sqrt{Q_F}} \right), \delta_{12} = \frac{\hat{T}}{Q_F^2}, \delta_{13} = \frac{\hat{T}}{6 Q_F},$$

$$\delta_{14} = \frac{\hat{S}}{2 Q_F} \left(1 - \frac{2}{\sqrt{Q_F} \text{Sinh} \sqrt{Q_F}} \right), \delta_{15} = \frac{\hat{S}}{Q_F^2}, \delta_{16} = \frac{\hat{S}}{6 Q_F}$$

and $\zeta_f = \frac{\alpha_{TF}}{\alpha_{TF}}$ represents ratio of the thermal expansion coefficients of fluid phase in porouslayer to the

thermal expansion coefficient with respect to fluid layer, $\zeta_s = \frac{\alpha_{TF}}{\alpha_{TF}}$ represents ratio of the thermal expansion

coefficient of solid phase in porous layer to the thermal expansion coefficient in the fluid layer, $\hat{\kappa}_{fP} = \frac{\kappa}{\kappa_{fP}}$

represents ratio of thermal diffusivity in fluid layer to fluid phase thermal diffusivity in the porous layer, $\hat{\kappa}_{sP} = \frac{\kappa}{\kappa_{sP}}$

represents ratio of thermal diffusivity in fluid layer to solid phase thermal diffusivity in the porous layer, $\hat{\kappa}_{cP} = \frac{\kappa}{\kappa_{cP}}$

5. Outcomes and discussions

The role of LTNE over the onset of DDRBM convection has been investigated. The critical Rayleigh numbers are attained and compared for both LTE and LTNE models by through Regular pertubation mode.

Parameters that favour LTNE precisely are, nothing but solid phase thermal expansion ratio ζ_s , solid phase thermal diffusivity ratio $\hat{\kappa}_{sP}$ and inter-phase thermal diffusivity ratio τ . Figures (2), (3) and (3) interpret the impact of these parameters on critical Rayleigh number keeping the other parameters fixed.

The effects of solid phase thermal expansion ratio ζ_s over critical Rayleigh number are represented in Figure-2 considering $\zeta_s = 2, 5$ and 10 . The curves are found diverging showing that it is sensitive when the double layered system is dominated by porous layer. Study reveals that the critical Rayleigh number decreases when ζ_s increases which destabilizes the system. Hence, there is quicker onset of DDRBM convection.

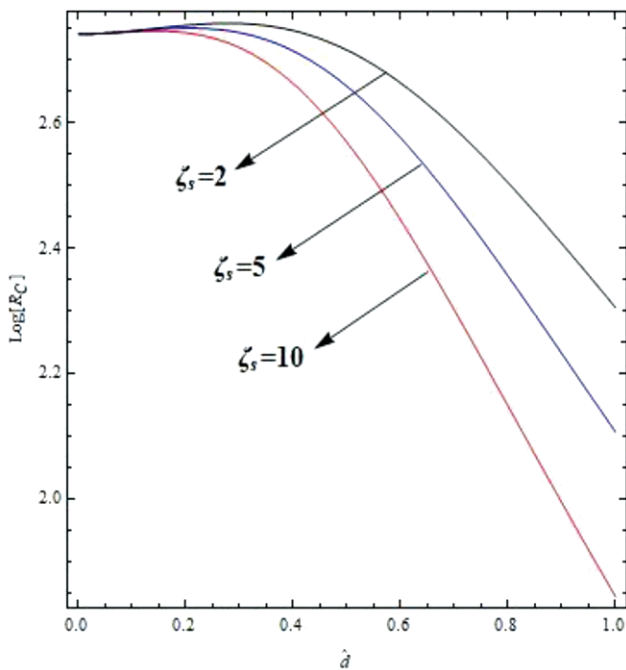


Figure 2

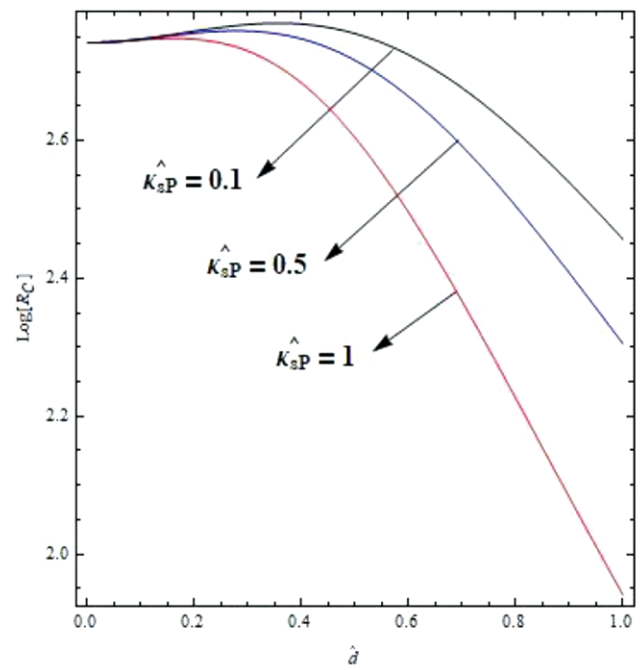


Figure 3

The effects of solid phase thermal diffusivity ratio $\hat{\kappa}_{sp}$ over critical Rayleigh number are depicted in figure-3 when $\hat{\kappa}_{sp} = 0.1, 0.5$ and 1 . Divergence is noticed from the figure and is evident that it is sensitive in double layered system dominated by porous layer. Also, decrease in critical Rayleigh number is noticed when $\hat{\kappa}_{sp}$ increases which destabilizes the system. Hence, onset of DDRBM convection is preponed.

The impact of inter-phase thermal diffusivity ratio τ over critical Rayleigh number are depicted in figure-4 for $\tau = 0.1, 0.5$ and 1 . The diverging curves indicate the sensitiveness of this parameter for the porous layer dominant double layered system. The study reveals that the critical Rayleigh number decreases when τ increases, thereby destabilizing the set-up. Hence onset of DDRBM convection occurs quickly.

Graphs have been presented for Critical Rayleigh number R_C against depth ratio \hat{d} for the fixed values of $\beta = 0.01, \zeta_f = 1, Q_F = 5, R_{SF} = 5, \hat{T} = 1, \tau_{cp} = 0.1$ and $\hat{\kappa}_{cp} = 0.1$. The outcome of altering each of the constraints such as fluid phase thermal expansion ratio ζ_p , Chandrasekhar number Q_F , Solute Rayleigh number R_{SP} , Thermal ratio \hat{T} , solute diffusivity ratio for porous layer τ_{cp} and thermal-solute diffusivity ratio for the porous layer with all other parameters unaltered is displayed for both LTNE & LTE models in figures (5), (6), (7), (8), (9), (10) and (11) respectively.

The effects of β , porous parameter on the critical Rayleigh number are shown in Figure-5. It is seen that

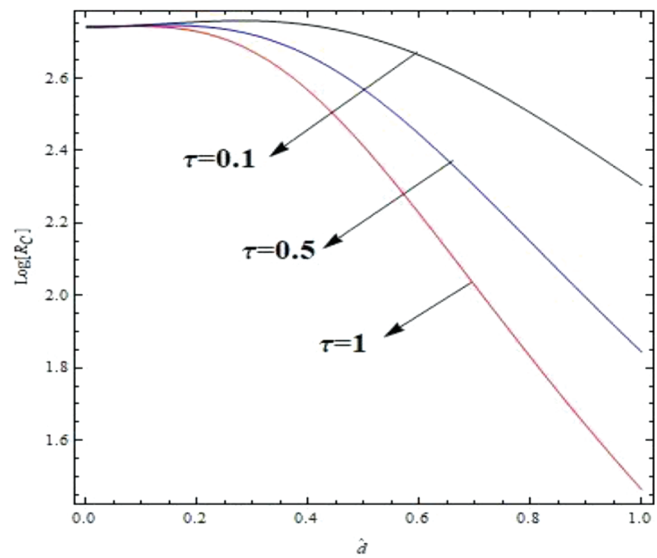


Figure 4

the curves are diverging with assigned values $\beta = 0.01, 0.7$ and 1 which proves that variation effect is protruding in case of double layered system with $d_F \ll d_p$. It is also evident from the figure that increase in β results into decrease in critical Rayleigh number and hence the set-up can be destabilized resulting in earlier onset of DDRBM convection. The critical Rayleigh numbers for LTNE model are smaller than those for the LTE Model, hence the role of LTNE is significant and

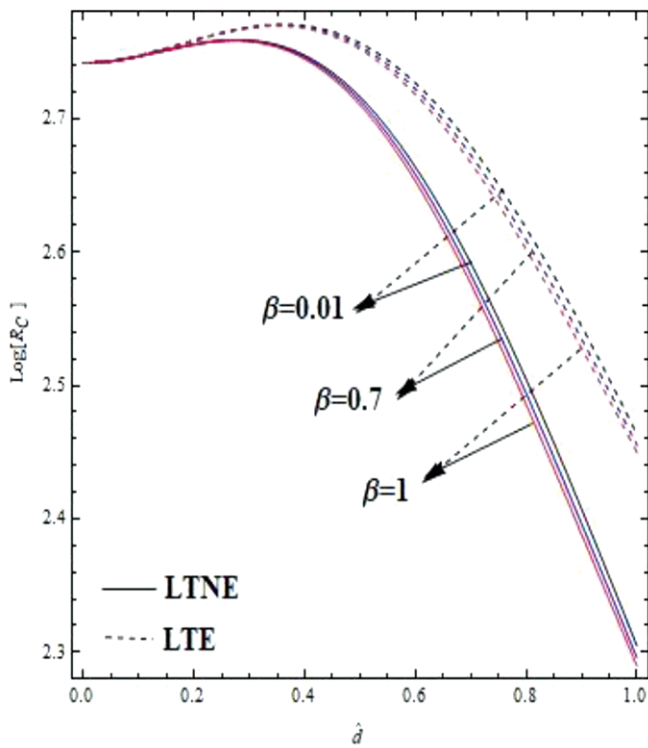


Figure 5

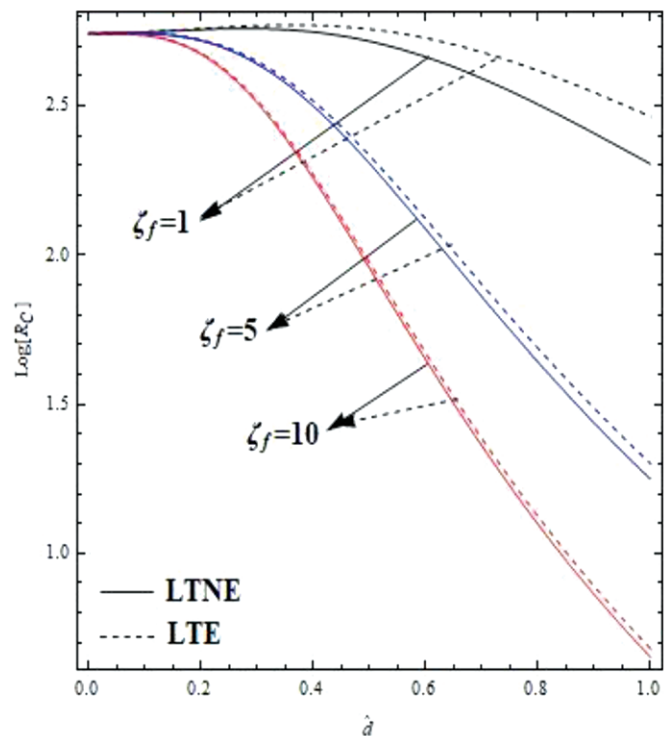


Figure 6

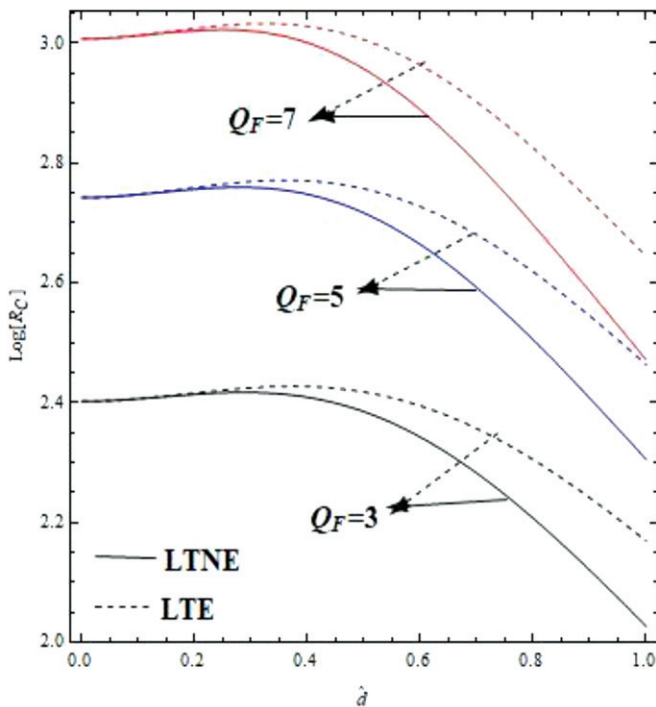


Figure 7

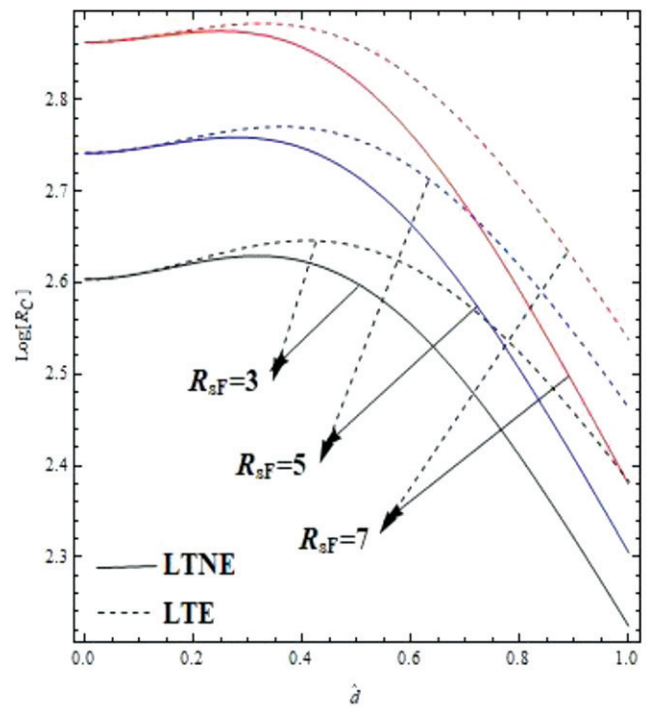


Figure 8

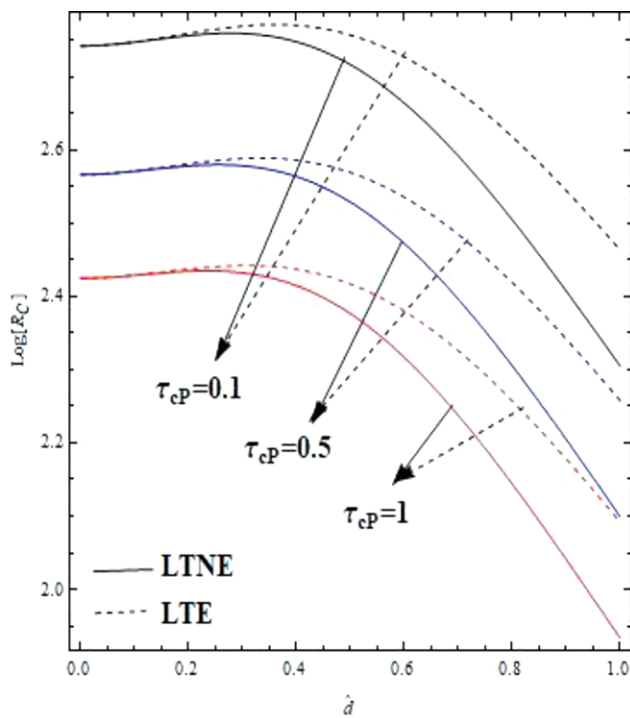


Figure 9

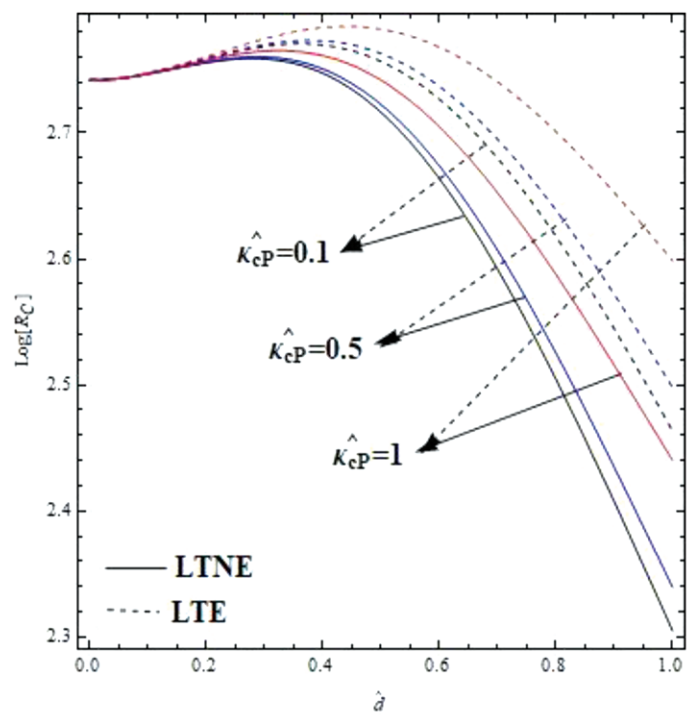


Figure 10

cannot be neglected in the situations where the convection has to be controlled.

The effects of ζ_f , fluid phase thermal expansion ratio on the critical Rayleigh number are shown in Figure-6. It is seen that the curves are diverging with assigned values $\zeta_f = 1, 5$ and 10 which proves that variation effect is protruding in case of double layer with $d_f \ll d_p$. It is also evident from the figure that increase in ζ_f results into decrease in critical Rayleigh number and hence the set-up can be destabilized. As this parameter increases the gap between LTNE and LTE decreases. Hence the prominence of LTNE is guaranteed at higher values of thermal expansion coefficient of fluid phase.

The effects of Chandrasekhar number Q_F over critical Rayleigh number are depicted in Figure-7 when $Q_F = 3, 5$ and 7 . The curves converge minutely and the observation using the graph is increase in critical Rayleigh number when Q_F increases for both LTNE and LTE. Hence the system gets stabilized thereby resulting in late onset of DDRBM convection.

The effects of solute Rayleigh number R_{SF} over critical Rayleigh number are depicted in Figure-8. In this case, minute convergence of the curves is noticed when $R_{SF} = 3, 5$ and 7 , indicating it is sensitive during dominance of porous layer over the double layer system. Increase in critical Rayleigh number is observed when R_{SF} increases. Hence the set-up is stable thereby delays the onset of DDRBM convection.

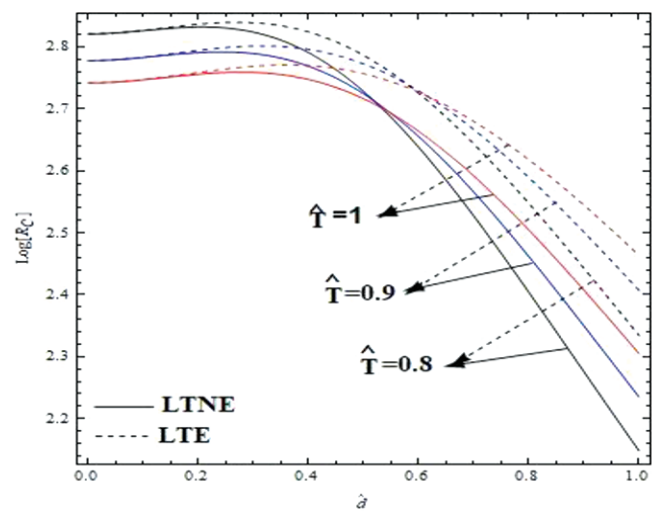


Figure 11

The effects of solute diffusivity ratio for porous layer τ_{cp} over critical Rayleigh number are displayed in Figure-9. In this case, neutral behaviour of the curves is noticed for values of $\tau_{cp} = 0.1, 0.5$ and 1 . Observation through the graph is decrease in critical Rayleigh number when τ_{cm} increases. Hence the set-up is destable which preponds the onset of DDRBM convection for both LTNE and LTE. LTNE remains to lead as long as the solute diffusivity in the porous layer is higher.

The influence of thermal-solute diffusivity ratio for the porous layer κ_{cp} on critical Rayleigh number are shown in Figure-10. In this case the curves are diverging for values of $\kappa_{cp} = 0.1, 1.5$ and 1 and variation effect protrudes in case of double layered system with $d_p \ll d_F$. It is noticed that critical Rayleigh number increases when κ_{cp} increases and thereby the system can be stabilised. That is the onset of DDRBM convection gets delayed. Retention of LTNE depends heavily on the thermal diffusivity with respect to porous layer.

The effects of thermal ratio \hat{T} over critical Rayleigh number are represented in Figure-11 for the values of $\hat{T} = 0.8, 0.9, 1$. In this case the dual behaviour is observed. The effect of this parameter relies emphatically on depth ratio. DDRBM convection sets in earlier for smaller values of depth ratio and reversible is the case for larger values of depth ratio. The critical Rayleigh numbers for LTNE are smaller when compared with those of LTE model. The LTNE model is plays a vital role during the situations, where in the convection has to kept under control.

Conclusions

- i. The critical Rayleigh numbers for LTE are higher than the same for LTNE model, hence the LTNE effects cannot be neglected in the situations where in the DDRBM Convection has to be controlled.
- ii. The onset of DDRBM convection is sensitive to the depth ratio and the effect of all the parameters in the study are dominant for larger values of depth ratio, i.e., for porous layer dominant double layered systems.
- iii. In the LTNE model, the smaller values of solid phase thermal expansion ratio, solid phase thermal diffusivity ratio and inter phase thermal diffusivity ratio are favourable for stability of the system, hence the onset of DDRBM convection can be postponed.
- iv. For both the LTNE and LTE models, Larger values of Chandrasekhar number, Solute Rayleigh numbers, thermal-solute diffusivity ratio, support the stability of the system.
- v. For both the LTNE and LTE models, Smaller values of Porous parameter, fluid phase thermal expansion ratio, solute diffusivity ratio for porous layer postpone the DDRBM Convection and hence support the stability of the system.
- vi. The impact of thermal ratio on the critical Rayleigh number relies emphatically on depth

ratio. DDRBM convection sets in earlier for smaller values of depth ratio and reversible is the case for larger values of depth ratio.

References

- [1] Abdelraheem Mahmoud Aly, Abdallah Aldosary, Ehab Mahmoud Mohamed, Double diffusion in a nanofluid cavity with a wavy hot source subjected to a magnetic field using ISPH method, Alexandria Engineering Journal (2021) 60, 1647–1664, 2021.
- [2] Asha Shivappa Kotnurkar and Sunitha Giddaiah, Double diffusion on peristaltic flow of nanofluid under the influences of magnetic field, porous medium, and thermal radiation, Engineering Reports, 2020;2:e12111. <https://doi.org/10.1002/eng2.12111>, 2020.
- [3] Ehrenstein U. and R. Peyret, A Chebyshev Collocation Method for the Navier-Stokes Equations with Application to Double-Diffusive Convection, International Journal for Numerical Methods in Fluids, Vol. 9, 427-452, 1989
- [4] Galenko P.K and D.A. Danilov, Local nonequilibrium effect on rapid dendritic growth in a binary alloy melt, Physics Letters A 235 (1997) 271-280, EISEVIER, 1997
- [5] Herbert E. Huppert and J. Stewart Turner, Double-diffusive convection, J. Fluid Mech. (1981), vol. 106, pp. 299-329, 1981
- [6] Hughes D. W and N. O. Weiss, Double-diffusive convection with two stabilizing gradients: strange consequences of magnetic buoyancy, J. Fluid Mech. (1995), vol. 301, pp. 383-406, 1995
- [7] Muhammad Bilal Riaz, Aziz Ur Rehman, Jan Awrejcewicz and Fahd Jarad, Double Diffusive Magneto-Free-Convection Flow of Oldroyd-B Fluid over a Vertical Plate with Heat and Mass Flux, Symmetry 2022, 14, 209. <https://doi.org/10.3390/sym14020209>, 2022
- [8] Pascale Garaud, Double-Diffusive Convection at Low Prandtl Number, Annual Review of Fluid Mechanics 2017.
- [9] Shashi Prabha Gogate S, Bharathi M.C , Ramesh B. Kudenatti, Heat transfer through mixed convection boundary layer in a porous medium: LTNE analysis, Applied Thermal Engineering 179 (2020) 115705, 2020.
- [10] Srinivasacharya D and G. Swamy Reddy, Double Diffusive Natural Convection in Power-Law Fluid Saturated Porous Medium with Soret and Dufour Effects, J. of the Braz. Soc. of Mech. Sci. &

- Eng., Vol. XXXIV, No. 4 / 525-530, 2012.
- [11] Sumithra R, Double Diffusive Magnetomarangoni Convection In A Composite Layer, International Journal of Application or Innovation in Engineering & Management (IJAIEM) Web Site: Volume 3, Issue 2, February 2014 ISSN 2319 -4847.
- [12] Sumithra R, N. Manjunatha, Analytical Study of Surface Tension Driven Magneto Convection in a Composite Layer Bounded by Adiabatic Boundaries, International journal of Engineering and innovative technology (IJEIT) 2277-3754, Vol. 1, pp. 249-257, 2012.
- [13] Sumithra R, N. Manjunatha, Effects of non-uniform temperature gradients on double diffusive marangoniconvection in a two layer system, International Journal of Pure and Applied Mathematics 118(2), DOI:10.12732/ijpam.v118i2.7
- [14] Sumithra R and Shyamala Venkatraman, Darcy-Benard Marangoni Convection in a Composite Layer Comprising of Couple Stress Fluid, International Journal of Applied Engineering Research, 15(7)(2020), 659-671.
- [15] Sumithra Ramakrishna, Basavarajappa Komala, Narayanappa Manjunatha, The onset of Darcy-Brinkman-Rayleigh-Benard convection in a composite system with thermal diffusion, Heat Transfer. 2021;1-17. wileyonlinelibrary.com/journal/ht.
-